Clinical Imaging 56 (2019) 114–123

Contents lists available at ScienceDirect

Clinical Imaging

journal homepage: www.elsevier.com/locate/clinimag

Molecular Imaging and Nuclear Medicine

Tumor-induced osteomalacia – Current imaging modalities and a systematic approach for tumor localization

Sampanna Jung Rayamajhi[a,*], Randy Yeh[b], Tony Wong[c], Shifali Dumeer[c], Bhagwant Rai Mittal[d], Fabrizio Remotti[e], Ijeuru Chikeka[e], Arun K. Reddy[d]

[a] Department of Radiology, NYU Langone Health, United States of America
[b] Department of Radiology, Memorial Sloan Kettering Cancer Center, United States of America
[c] Department of Radiology, New York-Presbyterian/Columbia University Medical Center, United States of America
[d] Department of Nuclear Medicine, Post Graduate Institute of Medical Education and Research, Chandigarh, India
[e] Department of Pathology, New York-Presbyterian/Columbia University Medical Center, United States of America

ARTICLE INFO

Keywords:
Tumor-induced osteomalacia (TIO)
Phosphaturic mesenchymal tumor
FGF23
Octreoscan
DOTATATE

ABSTRACT

Paraneoplastic syndromes are symptom complexes that cannot be readily explained by local or distant spread of the tumor. They can occur due to hormone production, autoimmunity or other biologically active products produced by the tumor, etc. Tumor induced osteomalacia is a rare paraneoplastic syndrome in which the manifestation is mainly musculoskeletal such as bone pain, fractures and muscle weakness as a consequence of elaboration of fibroblast growth factor 23 (FGF23) by the tumor.

Most of these tumors are solitary and small and hence localization of these tumors is often challenging. This review summarizes the various anatomic imaging modalities such as plain radiographs, computed tomography (CT), and magnetic resonance imaging (MRI) and nuclear medicine imaging techniques in the evaluation of these tumors.

1. Introduction

Paraneoplastic syndromes are a group of clinical manifestations that occur in conjunction with a neoplasm but are not directly caused by the mass effect of the tumor or its metastases, and are not a side effect of the medical treatment [1]. These syndromes are due to the production of substances by the neoplasm or are secondary to tumor associated immune reactions [1]. A rare paraneoplastic syndrome is the so-called tumor induced osteomalacia (TIO) or oncogenic osteomalacia (OO), in which the signs and symptoms of osteomalacia are due to phosphate wasting. Patients present with bone pain, fractures, renal phosphate wasting, hypophosphatemia, decreased serum 1,25-dihydroxyvitamin D3 levels, and resistance to vitamin D supplementation [2].

TIO is often a diagnostic challenge, as it is reflected by the generally long time-lag between onset of symptoms and final diagnosis. Most osteomalacia-inducing tumors are detected during the late fourth to the early fifth decades of life. They are usually located in the soft tissues and bones and tend to be solitary, although multifocal tumors have been reported. Because of their small size, they are typically not detected on physical examination and can be difficult to localize [3].

Most osteomalacia-inducing tumors are benign but malignant examples have been reported. The most common of these tumors is the so-called phosphaturic mesenchymal tumor (mixed connective tissue variant) (PMT-MCT) [2]. PMT-MCT is a rare, distinctive connective tissue neoplasm that typically is characterized by a distinctive admixture of spindle cells, osteoclasts-like giant cells, microcysts, prominent blood vessels, cartilage-like matrix, and grungy calcification [2]. In the majority of cases, the osteomalacia is secondary to the tumor cell production of fibroblast growth factor 23 (FGF23), a protein that is encoded by the FGF23 gene and is involved in the Vitamin D and phosphate metabolism [2]. The dysregulated production of this protein leads to systemic bone demineralization, primarily by inhibition of renal tubular epithelial phosphate transport. However, FGF 23 elevation is not specific of TIO and increased levels can also be found in other hypophosphatemic and osteomalacia-inducing musculoskeletal disorders, such as X-linked hypophosphatemic rickets (XLHR), and autosomal dominant and recessive hypophosphatemic rickets (ADHR and ARHR) [4].

The diagnostic process that accompanies a suspected tumor induced osteomalacia and guides the identification of the underlying neoplasm is often arduous. Once the aforementioned genetic disorders are excluded, the investigation requires a thorough biochemical evaluation of

* Corresponding author at: 515 w, 170 street, App 55, New York, NY 10032, United States of America.
E-mail address: Sampanna.Rayamajhi@nyulangone.org (S.J. Rayamajhi).

https://doi.org/10.1016/j.clinimag.2019.04.007
Received 6 January 2019; Received in revised form 27 March 2019; Accepted 15 April 2019
0899-7071/

the patient. In the presence of low serum levels of phosphorus secondary to renal phosphate wasting (due to decreased tubular reabsorption of phosphate), or if elevated levels of alkaline phosphatase are present with low or inappropriately normal values of 1,25-vitamin D, and if there is increase of the circulating levels of FGF23, it is likely that a phosphaturic mesenchymal neoplasm is responsible for the TIO. In the past few years, advances in medical imaging have enhanced the effective localization of osteomalacia-inducing tumors. In this review, we will discuss in detail the currently available functional and anatomical imaging modalities, their role in TIO and management, and propose a strategic approach for tumor localization.

2. Nuclear medicine imaging

2.1. Somatostatin receptor (SSTR)-analog imaging

Somatostatin is a 14-amino-acid cyclic neuropeptide mainly secreted by neurons and endocrine cells. Somatostatin receptors (SSTRs) are G-protein coupled receptors involved in various intracellular signaling pathways such as inhibition of adenylyl cyclase following hormone binding [5] and interaction with calcium and potassium channels. SSTRs are found on many cells of neuroendocrine origin and expressed on most neuroendocrine tumors and hence represent the basis for in vivo tumor imaging using somatostatin receptor analogs. However, SSTR expression is not specific to neuroendocrine tumors and SSTRs are also expressed in non-neuroendocrine tumors such as lymphomas, breast cancer, thyroid cancer etc. Although the primary indication of imaging with radiolabeled SSTR-analogs is for evaluation of neuroendocrine tumors, it has also been successfully used for staging of mesenchymal tumors such as sarcomas, which also express SSTRs [6]. Since most tumors associated with TIO are mesenchymal in origin and therefore express different SSTR subtypes, predominantly SSTR 2 [7–13], culprit tumors can be detected using single photon emission computed tomography (SPECT) or positron emission tomography (PET) based radiolabeled SSTR analogs (Table 1).

2.1.1. SPECT radiopharmaceuticals for SSTR imaging

Octreotide is a synthetic octapeptide analog of somatostatin that has a special binding affinity to somatostatin receptor SSTR 2 [14]. Indium 111-DTPA-octreotide or Octreoscan is the most commonly used functional imaging modality worldwide for the evaluation of SSTR–positive tumors and has also been used widely to locate osteomalacia inducing tumors [15]. Despite its popularity, Octreoscan has several major disadvantages including a relatively long radiopharmaceutical injection to scan time, images typically being acquired at two-time points, usually at 4 h and 24 h [16] and poor spatial resolution. Although whole-body SPECT/CT is technically feasible and allows three-dimensional imaging, the process is time-consuming and therefore acquisition of tomographic images is usually limited to areas of suspicious tracer uptake on planar imaging for lesion characterization, rather than a whole-body survey. Since Indium-111 has a long physical half-life of 2.8 days and emits high-energy gamma rays, SSTR imaging with Technetium-99m (Tc-99m)-labeled peptides have been used as an alternative, especially given greater availability, shorter half-life of 6 h, lower energy gamma rays and better imaging characteristics than Indium-111. Recently, Tc-99m-HYNIC-octreotide, a Tc-99m labeled somatostatin analog has been increasingly used and found to be very effective in the imaging of somatostatin receptor expressing tumors such as gastroenteropancreatic (GEP) neuroendocrine tumor as well as other non-GEP tumors overexpressing SSTR at various densities such as sarcomas, breast cancer, ovarian cancer, meningiomas etc. Although studies are limited, Tc-99m-HYNIC-octreotide scintigraphy has shown to be very useful to localizing osteomalacia-inducing tumors [17,18]. To our knowledge, the largest study evaluating TIO with Tc-99m-HYNIC-octreotide scintigraphy has shown the sensitivity of 86.3% and a specificity of 99.1% for detecting culprit tumors [19]. During Tc-99m-HYNIC- octreotide

Table 1
Nuclear medicine imaging modalities in evaluation of TIO.

Functional imaging modality	Radiopharmaceutical	PET/SPECT	Source	Mechanism of tracer localization in tumor
Somatostatin receptor imaging				
OCTREOSCAN	In-111-DTPA octreotide	Planar imaging + SPECT/CT	Cyclotron	SSTR 2,3 and 5 (predominantly SSTR 2)
HYNIC Scan	Tc99m-HYNIC-Tyl3-octreotide	CT	Tc-99m generator	Predominantly SSTR 2
DOTATATE Scan	Ga-68-DOTA-Tyr3-octreotate	PET/CT	Ge68/Ga68 generator	Predominantly SSTR 2
DOTANOC Scan	Ga-68-DOTA-Nal3-octreotide			SSTR 2, 5
DOTATOC Scan	Ga-68-DOTA-Tyl3-octreotide			SSTR 2,3,5
FDG Scan	F-18-FDG	PET/CT	Cyclotron	Glucose (GLUT-1) transporter
Sestamibi Scan	Tc-99m-Sestamibi (Tc-99m MIBI)	Planar imaging + SPECT/CT	Tc-99m generator	Tc-99m-Sestamibi accumulates within the mitochondria and cytoplasm of cells on the basis of electrical potentials generated across the membrane bilayers.
Thallium Scan	Tl-201	Planar imaging + SPECT/CT	Cyclotron	Multifactorial related to tumor blood flow, tumor viability, vascular immaturity with leakage, and increased cell membrane permeability
Bone scintigraphy (bone scan)	Tc-99m-diphosphonate (Tc-99m-MDP)	Planar imaging + SPECT/CT	Tc-99m generator	Chemisorption onto surface of bone trabeculae
Blood-pool scintigraphy	Tc-99m-labeled RBC	Planar imaging + SPECT/CT	Tc-99m generator	Tumor pooling of labeled RBC, possibly due to rich tumor vasculature of osteomalacia-inducing tumors.

scintigraphy, images are acquired after 4 h of tracer injection [20], which allows one-day imaging protocol, unlike Octreoscan. The estimated effective dose from a whole-body 99mTc-HYNIC- octreotide scan is estimated to be 4.6 mSv per scan [21] which is comparatively lower than an exposure of 0.08 mSv/MBq [22] or approximately 5.9 mSv per scan during Octreoscan. Physiological uptake of both In-111-DTPA-octreotide and Tc-99m-HYNIC- octreotide in the liver may make image interpretation difficult, although tumor-inducing osteomalacia located in the liver has only been rarely reported [23]. Pitfalls of both these SPECT agents include tracer uptake in inflammatory conditions such as arthritis [24], which might be mistaken for bone or soft tissue tumor. Nasal mucosal uptake may be seen in patients with a common cold in Octreoscan [25] and should not be confused for sino-nasal mesenchymal tumors, which are not uncommon in the region.

2.1.2. PET radiopharmaceuticals for SSTR imaging

Gallium-68 (Ga-68) is a positron-emitting radionuclide used in PET imaging. Ga-68 has a short half-life of 68 min and can be conveniently produced in a cyclotron-independent manner using a Ge-68/Ga-68 generator with a half-life of 270.8 days. The radioconjugate typically contains the radionuclide Ga-68, a chelator (DOTA) that links the radionuclide and one of the somatostatin analog peptides Tyr-3-octreotate (TATE), 1-Nal3-octreotide (NOC) or Tyr-3-octreotide (TOC). Each peptide has different affinity profiles for SSTR 1–5. Over the last few years, Ga-68 labeled somatostatin analog imaging has made a considerable impact in the management of neuroendocrine tumors. Similarly, its use in non-neuroendocrine tumors has also proved effective for imaging different tumors of the brain, meninges, thyroid, breast, prostate, melanoma etc. [26,27]. The three major Ga-68 labeled somatostatin analogs DOTATATE, DOTANOC [28] and DOTATOC [29] have all been successfully used to detect osteomalacia-inducing tumors. The higher affinity of DOTATATE for SSTR 2, the receptor subtype predominantly overexpressed, may favor its use in TIO over DOTANOC and DOTATOC. The results of Ga-68-DOTATATE PET/CT for localizing these tumors appears promising, with studies reporting high sensitivity ranging from 90 to 100% and specificity of 90.9% [30,31]. Current literature suggests the clear superiority of Ga-68-labeled peptides over Octreoscan [12] and F-18-FDG PET/CT [20,32,33] in detecting culprit tumors making it the imaging modality of choice whenever available (Fig. 1). Recently, a few studies have added a potential therapeutic dimension of Ga-68-DOTATATE in addition to its use for tumor localization. A recently published study highlighted the use of Ga-68-DOTATATE PET/CT-guided biopsy and cryoablation of an osteomalacia-inducing tumor [34]. Interestingly, Basu et al. recently described a case utilizing a theranostic approach using peptide receptor radionuclide therapy (PRRT) with Lutetium-177 (Lu-177)-DOTATATE, for a patient with a recurrent inoperable skull-based tumor following documentation of high somatostatin receptor expression by Ga-68-DOTATATE imaging resulting in symptomatic improvement [35]. However, PET imaging with Ga-68-DOTA-peptides has its own limitations. The expression of SSTR is not specific for tumors and has well been documented in inflammatory conditions such as sarcoidosis [36], inflammatory bowel disease [37], and rheumatoid arthritis [38], leading to false positive scans. Expression of SSTR by osteoblasts may lead to a non-tumor uptake in degenerative bone disease, fractures, fibrous dysplasia and vertebral hemangioma [39–41]. Since osteomalacia can frequently lead to insufficiency fractures, resulting in tracer uptake, this pitfall should be cautiously interpreted during Ga-68-DOTA-peptide imaging, and equivocal or doubtful lesions should be followed by regional MRI for further characterization. The main difference of Ga-68-DOTATATE is that the radionuclide is generator produced and does not need fasting prior to the scan, unlike conventional F-18-FDG which is cyclotron produced and needs fasting requirement prior to the scan. The radiation exposure of 4.8 mSv, 4.3 mSv and 3.1 mSv for Ga-68-DOTATATE, Ga-68-DOTATOC, and Ga-68-DOTANOC PET, respectively, is relative less than compared to of 5.9 mSv and 7.0 mSv for In-111-DTPA-octreotide and F-18 FDG PET imaging, respectively [42]. The excellent target-to-background ratio that Ga-68 PET provides is significantly higher as compared to F-18 FDG PET, consequently resulting in high standardized uptake values (SUVs) which may be an added advantage in the detection of small tumors. Although Ga-68 labeled somatostatin analogs have been available in several European countries for quite some time, Ga-68 DOTATATE has only been recently approved for imaging neuroendocrine tumors in the United States (NETSPOT) and many other countries. Therefore, availability of this modality and reimbursement issues might be a limiting factor for its use in evaluating TIO, especially in the lack of clear-cut guidelines for this indication. Ga-68 DOTA-peptide imaging for TIO requires modifications to the conventional PET/CT protocol. Instead of conventional imaging from the skull bases to mid-thighs, a vertex to toes protocol should be followed as most tumors occur in the lower extremities [43]. To decrease the chances of missing a tumor, we advocate a step-wise approach while reading whole-body images to find the culprit lesion. Since the pelvis and the lower extremities harbor approximately 50–60% of the tumors [2,44,45], we advocate a thorough evaluation of these areas first on the PET/CT images, both in CT soft tissue and bone windows. Following this, we begin a careful examination of the craniofacial region which accounts for nearly 30% of the lesions [44]. A thorough check of the sinonasal region and careful evaluation of the mandible, maxilla, gingiva, oral cavity, pharynx, larynx, and thyroid should be performed as these are sites have been reported to harbor tumors [25]. Then, a thorough survey of the thorax, abdomen and upper extremities is then undertaken. Potential pitfalls should always be considered while evaluating every region of the body (Table 2).

2.2. F-18 FDG PET/CT

F18-fluorodeoxyglucose (F-18 FDG) is the most widely used PET radiopharmaceutical worldwide for various oncological and non-oncological indications. Although most mesenchymal tumors, associated with oncogenic osteomalacia are benign in nature, studies have demonstrated a relatively high F-18 FDG uptake within these tumors, allowing their detection using FDG (Fig. 2). Although F-18 FDG PET/CT has shown high sensitivities for culprit tumor localization [46], comparative studies have shown F-18 FDG PET/CT to be inferior to Octreoscan, Tc-99m HYNIC TOC SPECT/CT and Ga-68 DOTATATE PET/CT in detecting culprit tumors [15,20]. F-18 FDG is a non-specific tracer and enters the cells expressing glucose transporters (GLUT-1). In addition to malignant cells, inflammatory cells also possess these transporters, which are upregulated in response to injury and trauma leading to detectable F-18 FDG uptake. Similar to Ga-68 DOTA-peptides, insufficiency fractures in patients with osteomalacia could lead to false positive interpretations on ^{18}F-FDG PET/CT scans [47]. Careful analysis of the F-18 FDG uptake using non-fused CT bone window might reveal the fracture line and avoid misdiagnosis. Other conditions leading to false positive F-18 FDG uptake requiring careful CT bone window evaluation include active arthropathies, degenerative changes, osteomyelitis, post-operative site uptake, tendonitis, and bone infarcts [47,48]. Culprit tumors are frequently found in the head and neck region [49], especially in the paranasal sinuses which are the most common location in this region and account for 5–10% of cases overall [2,44]. Intra-oral tumors constitute at least 24% of phosphaturic mesenchymal tumors in the head and neck, a majority of which lie in the mandible [50] and tumors are also found commonly in the maxilla, gingival, floor of mouth and tongue [45,50,51]. Since head and neck infections such as sinusitis, dental abscess, tonsillitis, and mastoiditis etc. are common and can lead to F-18 FDG uptake [52] and a falsely positive study [46], any tracer uptake in the region should be cautiously evaluated. Also an inherent disadvantage with FDG is the non-specific muscular uptake due to various reasons such as exercise, muscle strain or hyperinsulinemia which can potentially mask the tumors located

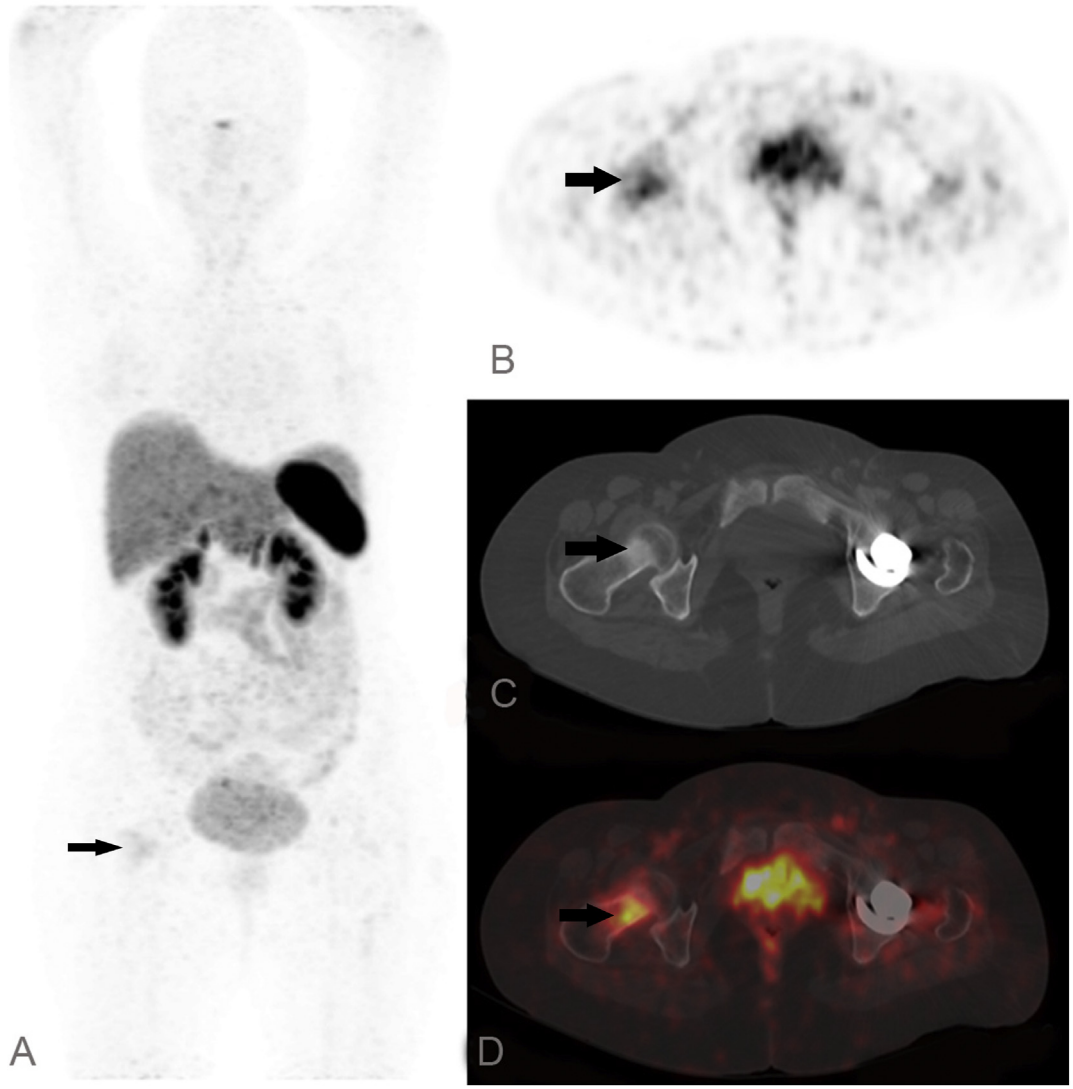

Fig. 1. 44-Year-old female with generalized muscle aches. FGF 23 was elevated (339 RIU/ml). Ga-68 DOTATATE images (A) Maximum intensity projection images and (B) axial PET images, show abnormal focal tracer uptake in the region of right femoral neck, SUV 8.0. Physiological tracer uptake is seen in the pituitary, liver and spleen with excretion of tracer through the kidneys. (C) Transaxial CT and (D) fused PET/CT localize the increased tracer uptake to a sclerotic lesion in the right femoral neck, which was later pathologically consistent with phosphaturic mesenchymal tumor.

adjacent to muscles. It may also be prudent to use intravenous contrast in PET protocols to demonstrate features such as contrast enhancement in the tumor [46] and outline its extent for planning surgery, with the goal to attain tumor-free surgical margins to avoid recurrence. A puff-cheek-view, which is often used in oral cancer patients should be used to avoid PET reporting difficulties in the oral cavity and mis-interpretations due to the spilling of tracer activity and also to reduce dental artifacts [53,54]. Compared to SSTR PET imaging the major disadvantage of F-18 FDG PET is the fasting requirement of 4–6 h prior to the scan. Since tumors are likely to be missed during the standard-field imaging protocol, a vertex-to-toe FDG protocol should be followed, similar to a Ga-68 DOTATATE scan [55]. Before injection of F-18 FDG, a thorough history of trauma, recent infection in the head and neck, and recent tooth extraction is taken as these can lead to focal F-18 FDG uptake [56], Additionally, patients are strictly advised to avoid talking or chewing to avoid uptake in the tongue and masticatory muscles. As with other tumors, dental implants create a problem with PET/CT imaging of the head and neck by creating streak artifact and areas of increased activity. Given the high prevalence of TIO in the head and neck and the small sizes of most tumors, interpretation may be difficult. Therefore, careful evaluation of the non-attenuation corrected PET images may be helpful and a regional contrast-enhanced MRI may be a useful adjunct in difficult cases.

2.3. Other nuclear medicine imaging techniques

2.3.1. Tc-99m Sestamibi and Thallium-201 (Tl-201)

Since its introduction, Tc-99m sestamibi has been shown to be of value in the evaluation of many tumors including bone and soft tissue tumors, CNS neoplasm, breast cancers etc. and few reports have successfully demonstrated its utility in TIO [57–59]. Although comparison studies are limited, Ferraz et al. performed Tc-99m sestamibi and Octreoscan in four cases of suspected oncogenic osteomalacia and both modalities detected tumors in all patients [16]. This could be a very useful cost-effect method for detection of the tumor, especially in centers where Octreoscan or PET pharmaceuticals are not available but sestamibi kits are available for other routine nuclear medicine studies such as myocardial perfusion imaging and parathyroid imaging. A disadvantage of this scan is the low lesion-to-background ratio, making it difficult for image interpretation. Also, sestamibi is non-specific tumor agent, with uptake seen in benign skeletal lesions, such as fracture, osteomyelitis, diabetic foot etc. and might lead to a false positive

Table 2
Pearls and pitfalls in TIO imaging.

Pelvis and lower extremities
Pearls:
Comprise of 50–60% tumors, the majority are in the lower extremities.
Most lesions are eccentric and are located in the epiphysis of long bones.
Imaging protocol should include entire lower extremities, including the toes to avoid missing of tumors.
Osteomalacia may lead to subcapital fractures and femoral neck fractures, MRI can be helpful in suspicious cases.
Careful evaluation is necessary for areas of prior curettage in long bones as recurrence is not infrequent.
Pitfalls:
Insufficiency fractures are common in the pelvis, especially in the sacrum, might lead to false positives during functional imaging.
Head and neck
Pearls:
Comprise of 20–30% tumors.
The majority are located in the paranasal sinuses followed by the mandible.
Anterior cranial fossa needs careful assessment.
Puff cheek view may make PET/CT interpretations in the oral region easy.
Dental metallic implants may create artifacts causing PET/CT interpretation difficult, non-attenuation corrected images may help to interpret PET results better.
Pitfalls:
MRI features of osteomalacia-inducing tumors may be similar to meningiomas. Furthermore, meningiomas also express SSTR, hence are positive on somatostatin receptor imaging.
Potential site for F-18 FDG or Ga-68 labeled peptide PET/CT interpretation pitfalls, such as dental and paranasal sinus infections.
Thorax and abdomen
Pearls:
Comprise of 5–17% tumors.
CT of lungs is valuable as lung metastasis is not infrequent, especially in recurrent tumors.
Pitfalls:
Fracture of the ribs is extremely common in osteomalacia owing to poor mineral density. Fractures lead to a focal uptake in the bone scan, any uptake in the ribs should not misguide the search for a primary osteomalacia-inducing tumor.
Upper extremities
Pearls:
Comprise of 5–15% tumors.
Entire upper extremities should be included in the field of view, to avoid missing of tumors.
Pitfalls:
Cautious interpretation of false positive during functional imaging such as fractures, inflammatory disease of the joints.
Bone mineral density (BMD) recovery may be prolonged as compared to other sites even after tumor resection.
Muscular uptake may mask tumor uptake in F-18 FDG PET/CT.

study [60,61]. Like sestamibi, Thallium-201(Tl-201) has also been employed for tumor imaging of breast cancer, lymphomas, CNS tumor etc. and has also been used to detect tumors causing oncogenic osteomalacia [59]. It is also a non-specific tumor agent and Tl-201 uptake has been described in benign lesions including fractures [62].

2.3.2. Bloodpool scintigraphy

Technetium-99m bloodpool scintigraphy has also been used to detect possible tumors causing osteomalacia. Few studies have used whole-body Technetium-99m RBC blood pool scintigraphy to locate the causative tumors in patients with TIO [63,64]. The rationale of it use mainly lies in the fact that these tumors elaborate intrinsic microvasculature with an admixture of vessel size and vascular pattern [2], possibly leading to tracer pooling due to increased vascularity of the tumor. Since PMTMCT have a wide histological spectrum, it is unlikely that small tumors without a rich vascular supply will be diagnosed by this modality. Although the modality appears to be very cost-effective, image interpretation may be difficult owing to the low tumor-to-background ratio of the radiotracer, poor spatial resolution of planar scintigraphy, and poor localization of very small tumors.

2.3.3. Bone scintigraphy (bone scan)

Bone scintigraphy is a well-established imaging modality for the evaluation of a variety of pathologies involving skeletal metabolism such as osteomalacia, Paget's disease, and osteoporosis. While whole body bone scan is not specific to detect osteomalacia-inducing tumors, due to its high sensitivity it can be used as a skeletal survey for detecting osteomalacia-induced skeletal complications and serve as a basis for follow-up after therapeutic intervention.

The non-specific bone scan findings of metabolic bone disease such as increased tracer uptake by the mandible, vertebral column and the sternum creating the “tie sign”, are also found in tumor-induced osteomalacia [65]. Multiple areas of focally increased tracer uptake representing pseudofractures may be seen [66], which might mislead the effort to localize the occult primary tumor. Bone scan is sensitive in detecting more number of lesions, such as additional fracture sites than found with conventional radiography. Increased tracer uptake may be seen in areas such as the sacro-iliac joints, representing insufficiency fractures [67]. Although pseudofracture detection may be the most useful application of bone scintigraphy in TIO patients, scans showing a prominent appearance of the costochondral junction creating the ‘rachitic rosary sign’ and increased tracer uptake in the growth plates of are considered to be more specific of TIO [65,68,69] and should raise its suspicion if detected.

3. Anatomical imaging

3.1. Plain radiography and dual-energy X-ray absorptiometry (DXA)

Radiography and Dual-energy X-ray absorptiometry (DEXA) help to diagnose osteomalacia in patients with TIO which results from the disturbance of mineralization kinetics and increased bone resorption by osteoclasts. Since most osteomalacia-inducing tumors are eccentric and located in the epiphysis [70], any such lesion in the long bones on radiography should raise a suspicion of a possible tumor. Although radiographs may be helpful in tumor localization (Fig. 3) are usually noncontributory in tumor localization, they are extremely helpful in diagnosing complications such as fractures.

Besides locating the tumor, DEXA is helpful in patient follow up to evaluate recovery of bone mineral density. While surgical tumor resection may lead to dramatic improvement and complete resolution of symptoms, there is a time-lag in the improvement of bone mineral density, making the bones still prone to fractures [71]. Interestingly few studies have shown that the gain in bone density may be slower for radius as compared to femur and spine in TIO patients [72,73]. Following interventions, like other pathologies impacting bone mineralization, radiography may be useful to demonstrate bone healing and follow-up DEXA may be useful to demonstrate improvement in bone density [73,74].

3.2. Magnetic resonance imaging

Magnetic resonance imaging (MRI) has inherently superior soft tissue contrast to better characterize the soft tissue and bones, and therefore MRI skeletal survey has been frequently used to detect osteomalacia-inducing tumors [75,76]. Although different sequences have been defined, Short-tau inversion recovery (STIR) images show areas of high signal intensity to localize tumors [75] and should be used preferentially for suspected PMT [77]. T2-weighted fat-suppressed MR images (Fig. 4) is an alternative sequence for demonstrating tumors [78]. Like any whole-body imaging technique whole-body MRI has the advantage of detecting multifocal tumors throughout the body, although multifocal lesions are very rare in TIO [79]. Compared to other whole-body modalities, whole-body MRI is time-consuming and regional MRI can instead be considered to further characterize lesions detected on functional imaging (Table 1). Currently, the role of MRI is more on anatomically defining the tumor prior to surgery after

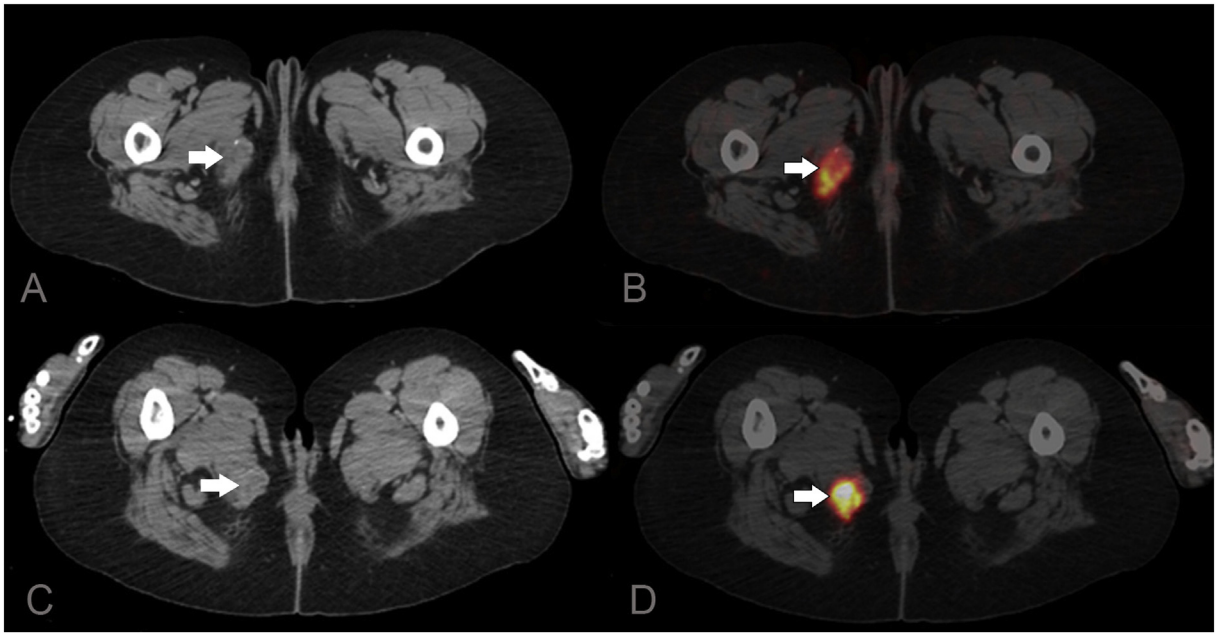

Fig. 2. 40-Year-old female with bone pains and proximal myopathy. (A) Transaxial CT (B) fused FDG PET/CT (C) transaxial CT and (D) fused Ga-68 DOTATATE PET/CT localizing radiotracer uptake within a soft tissue lesion in the right posterior thigh. The lesion demonstrates standardized uptake values of SUV 8.3 and SUV 18.2 on FDG and Ga-68 DOTATATE, respectively. Pathology was consistent with phosphaturic mesenchymal tumor.

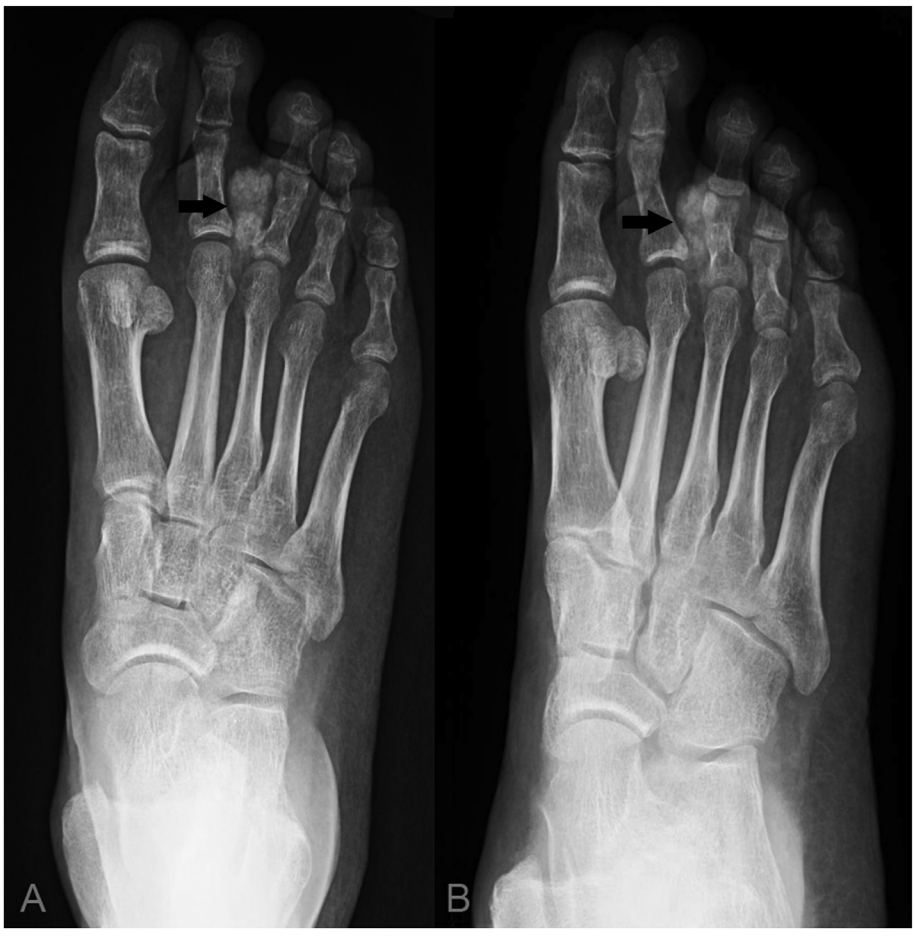

Fig. 3. 66-Year-old male with osteomalacia. (A) Anteroposterior and (B) oblique radiographs of the right foot, reveals a calcified lesion in the second web measuring approximately 2.9 × 2.1 cm. The second and third digits are splayed without erosion or bone destruction. The preoperative T-score at the right femoral trochanter was −3.1 and the bone marrow density (BMD) was 0.67 g/cm^2. Surgical resection revealed phosphaturic mesenchymal tumor. One year post resection of the tumor, T score of right femoral trochanter improved with T score of −0.5 and BMD 0.86 g/cm^2.

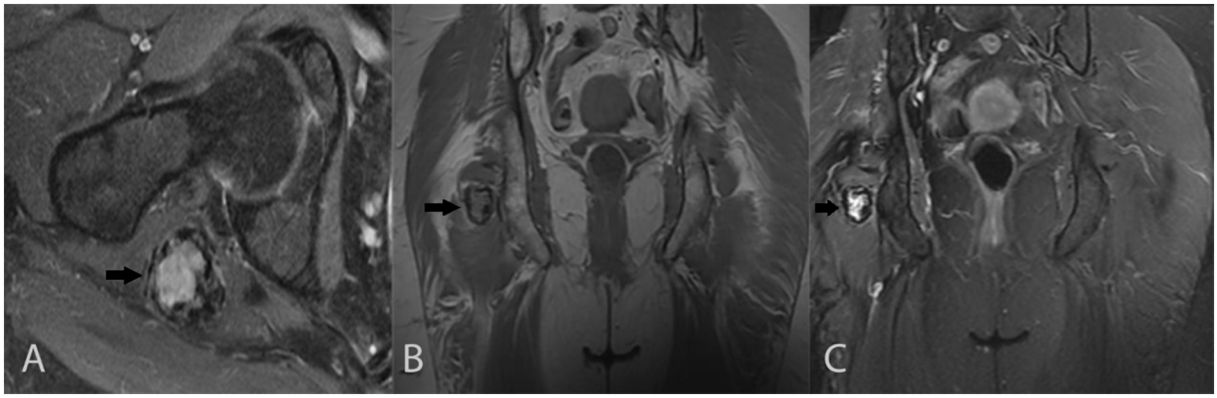

Fig. 4. 67-Year-old female with osteomalacia. (A) Axial T2 fat-suppressed, (B) coronal T1, (C) coronal T1 fat-suppressed post contrast images demonstrate a well-circumscribed rounded, deep soft tissue mass adjacent to the right ischial tuberosity measuring 2.7 cm. The mass demonstrates peripheral T1 and T2 hypointensity, most likely representing ossification, with internal T2 hyperintensity. Excision of the lesion was consistent with phosphaturic mesenchymal tumor.

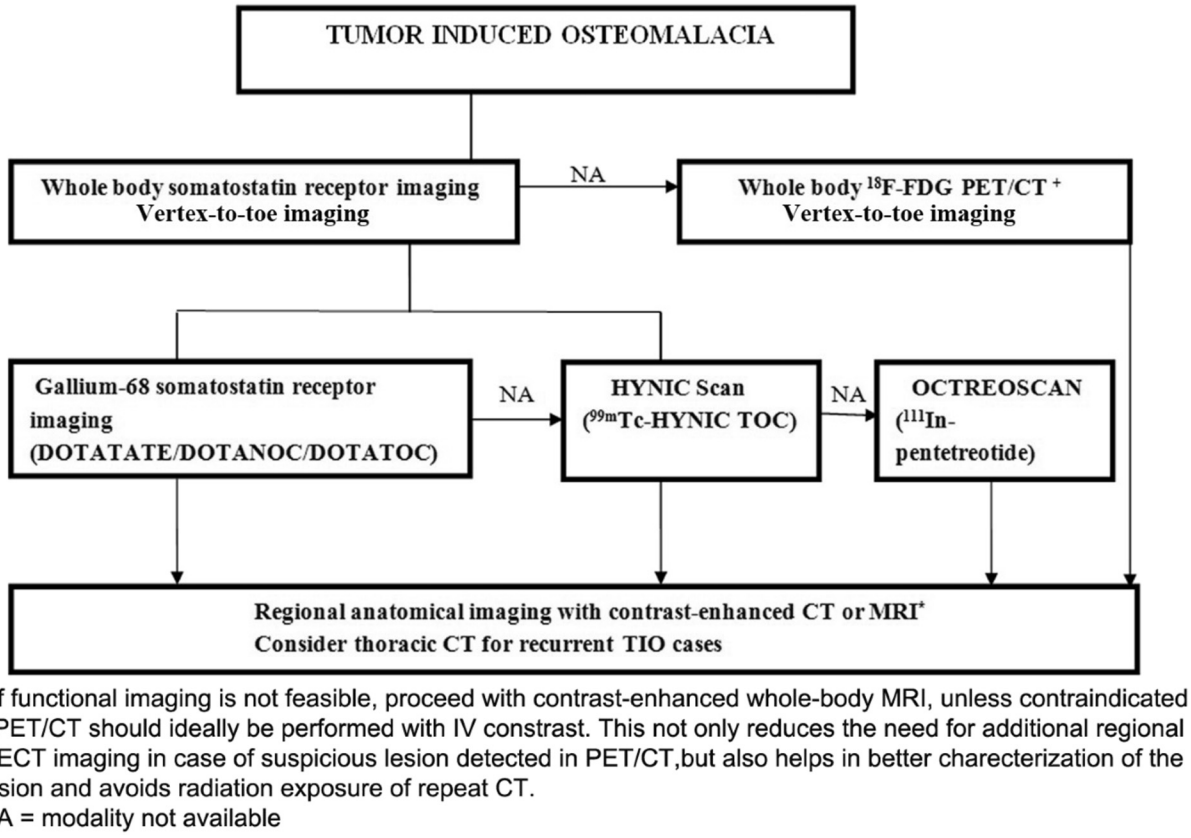

Fig. 5. Proposed imaging flow chart for localization of tumor using different modalities.

functional imaging has identified a possible culprit tumor. MRI is extremely useful to define the extent of the tumor for preoperative planning, in order to attain wide negative margins and thus prevent local recurrence. This is especially important in sinonasal tumors, as contrast MRI can delineate tumors accurately and identify extension to critical structures such as the cavernous sinus and orbit.

Interestingly, a few cases of intra-cranial osteomalacia inducing-tumors have also been reported, particularly in the anterior cranial fossa where contrast-enhanced MRI has proven to be extremely useful [80,81]. Osteomalacia-inducing tumors in the anterior cranial fossa may be mistaken for meningiomas in MRI, since they tend to be extra-axial, well circumscribed and demonstrate contrast enhancement. The presence of fat density may suggest the possibility of a phosphaturic mesenchymal tumors rather than a meningioma [80]. MRI may also be beneficial in tumor follow-up after surgery, since nuclear medicine imaging techniques can show false uptake of tracer [82] during inflammation and tissue healing. Sahoo et al. reported a very interesting case where FGF 23 levels were persistently elevated despite resection of an FDG avid PMTMCT from the tibia. An MRI of a non-FDG avid subcutaneous lesion was suspicious and following its resection, FGF 23 subsequently normalized. In their report, the non-FDG avid lesion was also PMTMCT but showing an osteoid-like matrix [83]. PMTMCTs containing osteoid-like matrix is a well- known entity [2], and whether this subtype is always non-FDG avid, should be further studied. MRI can also detect complications of TIO, such as bilateral insufficiency subchondral fractures of the femoral head [84], which may sometimes be difficult to appreciate by other imaging modalities.

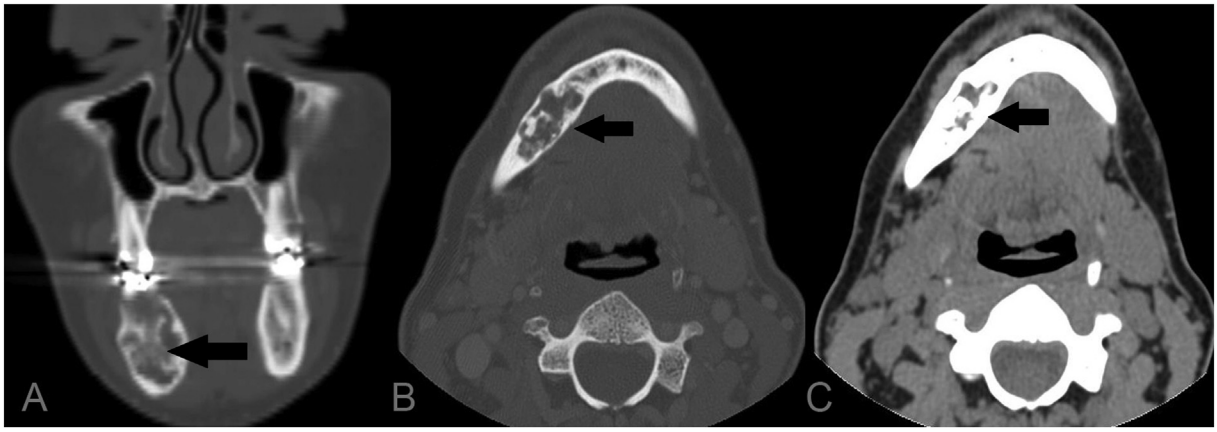

Fig. 6. 52-Year-old female with tumor induced osteomalcia. (A) Coronal CT (B) transaxial bone window and (C) transaxial soft tissue window reveals a mildly expansile lytic/sclerotic lesion in the mandible on the right. Pathology was consistent with phosphaturic mesenchymal tumor.

3.3. Computed tomography

Computed tomography (CT) has a limited role in localizing the culprit tumor. Similar to MRI, any area found suspicious during functional imaging may be further evaluated with CT, especially in institutions where hybrid functional and anatomical imaging with SPECT/CT or PET/CT is not available (Fig. 5). Since the paranasal sinuses are common sites for harboring these tumors, regional head and neck CT may sometimes be helpful to detect tumors in these areas (Fig. 6). Chest CT may also be helpful, as the lungs are a common site for metastasis [2,68,85–87]. This is particularly important in recurrent tumors, which are associated with increased risk of lung metastasis [2,45,88,89]. Besides helping in locating the culprit tumor, both CT and MRI-guided minimally invasive procedures such as cryoablation, ethanol and radiofrequency ablation have been successfully utilized in patients who decline surgical removal of the tumor, or in patients who are poor surgical candidates due to the complexity of surgery [90–93].

4. Future prospective

Combined positron emission tomography with magnetic resonance imaging (PET/MRI) is an evolving hybrid imaging modality with potential in imaging of TIO, given the superior contrast resolution of MRI over CT in bones and soft tissue, including the subcutaneous region. Recent studies have shown its superiority over ^{18}F-FDG PET/CT in detecting occult primary tumors as well as better characterizing the lesions showing tracer uptake [94]. Characterization of lesions showing abnormal radiotracer uptake is of paramount importance before labeling them as culprit tumors causing TIO, which is especially difficult for soft tissue lesions by PET/CT imaging owing to its poor soft tissue resolution. The synergism of MRI and PET providing vastly superior quality images than PET/CT for lesion characterization coupled with the fact that MRI has no radiological exposure may make PET/MRI a potential one-stop imaging modality to locate osteomalacia-inducing tumors. PET/MRI has also been found useful in somatostatin receptor expressing tumors imaging using ^{68}Ga-labeled peptides [95], and somatostatin receptor PET/MRI may prove to be effective for detection of osteomalacia-inducing tumors in the future.

References

[1] Kumar V, Abbas AK, Aster JC. Robbins and Cotran pathologic basis of disease. 9th ed. Philadelphia, PA: Elsevier/Saunders; 2015. [1391 p].
[2] Folpe AL, Fanburg-Smith JC, Billings SD, Bisceglia M, Bertoni F, Cho JY, et al. Most osteomalacia-associated mesenchymal tumors are a single histopathologic entity: an analysis of 32 cases and a comprehensive review of the literature. Am J Surg Pathol 2004;28(1):1–30.
[3] El-Maouche D, Sadowski SM, Papadakis GZ, Guthrie L, Cottle-Delisle C, Merkel R, et al. (68)Ga-DOTATATE for tumor localization in tumor-induced osteomalacia. J Clin Endocrinol Metab 2016;101(10):3575–81.
[4] Ramon I, Kleynen P, Body JJ, Karmali R. Fibroblast growth factor 23 and its role in phosphate homeostasis. Eur J Endocrinol 2010;162(1):1–10.
[5] Schonbrunn A. Somatostatin receptors present knowledge and future directions. Ann Oncol 1999;10(Suppl. 2):S17–21.
[6] Ferrari S, Dondi M, Fanti S, Zoboli S, Giacomini S, Mercuri M, et al. Somatostatin receptor (SSTR) scintigraphy in patients with osteosarcoma. Cancer Biother Radiopharm 2003;18(5):847–51.
[7] Jan de Beur SM, Streeten EA, Civelek AC, McCarthy EF, Uribe L, Marx SJ, et al. Localisation of mesenchymal tumours by somatostatin receptor imaging. Lancet 2002;359(9308):761–3.
[8] Ishii A, Imanishi Y, Kobayashi K, Hashimoto J, Ueda T, Miyauchi A, et al. The levels of somatostatin receptors in causative tumors of oncogenic osteomalacia are insufficient for their agonist to normalize serum phosphate levels. Calcif Tissue Int 2010;86(6):455–62.
[9] Houang M, Clarkson A, Sioson L, Elston MS, Clifton-Bligh RJ, Dray M, et al. Phosphaturic mesenchymal tumors show positive staining for somatostatin receptor 2A (SSTR2A). Hum Pathol 2013;44(12):2711–8.
[10] Reubi JC, Waser B, Laissue JA, Gebbers JO. Somatostatin and vasoactive intestinal peptide receptors in human mesenchymal tumors: in vitro identification. Cancer Res 1996;56(8):1922–31.
[11] Clifton-Bligh RJ, Hofman MS, Duncan E, Sim Ie W, Darnell D, Clarkson A, et al. Improving diagnosis of tumor-induced osteomalacia with Gallium-68 DOTATATE PET/CT. J Clin Endocrinol Metab 2013;98(2):687–94.
[12] Breer S, Brunkhorst T, Beil FT, Peldschus K, Heiland M, Klutmann S, et al. 68Ga DOTA-TATE PET/CT allows tumor localization in patients with tumor-induced osteomalacia but negative 111In-octreotide SPECT/CT. Bone 2014;64:222–7.
[13] Seufert J, Ebert K, Muller J, Eulert J, Hendrich C, Werner E, et al. Octreotide therapy for tumor-induced osteomalacia. N Engl J Med 2001;345(26):1883–8.
[14] Reubi JC, Waser B, Schaer JC, Laissue JA. Somatostatin receptor sst1-sst5 expression in normal and neoplastic human tissues using receptor autoradiography with subtype-selective ligands. Eur J Nucl Med 2001;28(7):836–46.
[15] Chong WH, Andreopoulou P, Chen CC, Reynolds J, Guthrie L, Kelly M, et al. Tumor localization and biochemical response to cure in tumor-induced osteomalacia. J Bone Miner Res Off J Am Soc Bone Miner Res 2013;28(6):1386–98.
[16] Ferraz MP, Watanabe T, Sado HN, Ono CR, Buchpiguel CA, Correa PH, et al. Concordance between whole-body scintigraphy 111In-octreotide and 99mTc-sestamibi uptake in the detection of four tumor-induced osteomalacia cases. J Clin Endocrinol Metab 2014;99(3):699–700.
[17] Jing H, Li F, Zhong D, Zhuang H. 99mTc-HYNIC-TOC (99mTc-hydrazinonicotinyl-Tyr3-octreotide) scintigraphy identifying two separate causative tumors in a patient with tumor-induced osteomalacia (TIO). Clin Nucl Med 2013;38(8):664–7.
[18] Jin X, Jing H, Li F, Zhuang H. Osteomalacia-inducing renal clear cell carcinoma uncovered by 99mTc-Hydrazinonicotinyl-Tyr3-octreotide (99mTc-HYNIC-TOC) scintigraphy. Clin Nucl Med 2013;38(11):922–4.
[19] Jing H, Li F, Zhuang H, Wang Z, Tian J, Xing X, et al. Effective detection of the tumors causing osteomalacia using [Tc-99m]-HYNIC-octreotide (99mTc-HYNIC-TOC) whole body scan. Eur J Radiol 2013;82(11):2028–34.
[20] Jadhav S, Kasaliwal R, Lele V, Rangarajan V, Chandra P, Shah H, et al. Functional imaging in primary tumour-induced osteomalacia: relative performance of FDG PET/CT vs somatostatin receptor-based functional scans: a series of nine patients. Clin Endocrinol (Oxf) 2014;81(1):31–7.
[21] Grimes J, Celler A, Birkenfeld B, Shcherbinin S, Listewnik MH, Piwowarska-Bilska H, et al. Patient-specific radiation dosimetry of 99mTc-HYNIC-Tyr3-octreotide in neuroendocrine tumors. J Nucl Med 2011;52(9):1474–81.
[22] Krenning EP, Bakker WH, Kooij PP, Breeman WA, Oei HY, de Jong M, et al. Somatostatin receptor scintigraphy with indium-111-DTPA-D-Phe-1-octreotide in man: metabolism, dosimetry and comparison with iodine-123-Tyr-3-octreotide. J Nucl Med 1992;33(5):652–8.
[23] Seijas R, Ares O, Sierra J, Perez-Dominguez M. Oncogenic osteomalacia: two case

reports with surprisingly different outcomes. Arch Orthop Trauma Surg 2009;129(4):533–9.
[24] Gabriel M, Decristoforo C, Donnemiller E, Ulmer H, Watfah Rychlinski C, Mather SJ, et al. An intrapatient comparison of 99mTc-EDDA/HYNIC-TOC with 111In-DTPA-octreotide for diagnosis of somatostatin receptor-expressing tumors. J Nucl Med 2003;44(5):708–16.
[25] Deep NL, Cain RB, McCullough AE, Hoxworth JM, Lal D. Sinonasal phosphaturic mesenchymal tumor: case report and systematic review. Allergy Rhinol (Providence) 2014;5(3):162–7.
[26] Sollini M, Erba PA, Fraternali A, Casali M, Di Paolo ML, Froio A, et al. PET and PET/CT with 68gallium-labeled somatostatin analogues in non GEP-NETs tumors. TheScientificWorldJournal 2014;2014:194123.
[27] Jung RS, Mittal BR, Bal A, Dey P, Shukla J, Kapoor R. Metastatic melanoma to the thyroid gland expressing somatostatin receptors-imaging with 68Ga-DOTANOC PET/CT. Clin Nucl Med 2015;40(2):175–6.
[28] Hesse E, Moessinger E, Rosenthal H, Laenger F, Brabant G, Petrich T, et al. Oncogenic osteomalacia: exact tumor localization by co-registration of positron emission and computed tomography. J Bone Miner Res Off J Am Soc Bone Miner Res 2007;22(1):158–62.
[29] Haeusler G, Freilinger M, Dominkus M, Egerbacher M, Amann G, Kolb A, et al. Tumor-induced hypophosphatemic rickets in an adolescent boy–clinical presentation, diagnosis, and histological findings in growth plate and muscle tissue. J Clin Endocrinol Metab 2010;95(10):4511–7.
[30] Zhang J, Zhu Z, Zhong D, Dang Y, Xing H, Du Y, et al. 68Ga DOTATATE PET/CT is an accurate imaging modality in the detection of culprit tumors causing osteomalacia. Clin Nucl Med 2015;40(8):642–6.
[31] Bhavani N, Reena Asirvatham A, Kallur K, Menon AS, Pavithran PV, Nair V, et al. Utility of Gallium-68 DOTANOC PET/CT in the localization of tumour-induced osteomalacia. Clin Endocrinol (Oxf) 2016;84(1):134–40.
[32] Agrawal K, Bhadada S, Mittal BR, Shukla J, Sood A, Bhattacharya A, et al. Comparison of 18F-FDG and 68Ga DOTATATE PET/CT in localization of tumor causing oncogenic osteomalacia. Clin Nucl Med 2015;40(1):e6–10.
[33] El-Maouche D, Sadowski SM, Papadakis GZ, Guthrie L, Cottle-Delisle C, Merkel R, et al. 68Ga-DOTATATE for tumor localization in tumor-induced osteomalacia. J Clin Endocrinol Metab 2016;101(10):3575–81.
[34] Maybody M, Grewal RK, Healey JH, Antonescu CR, Fanchon L, Hwang S, et al. Ga-68 DOTATOC PET/CT-guided biopsy and cryoablation with autoradiography of biopsy specimen for treatment of tumor-induced osteomalacia. Cardiovasc Intervent Radiol 2016;39(9):1352–7.
[35] Basu S, Fargose P. 177Lu-DOTATATE PRRT in recurrent skull-base phosphaturic mesenchymal tumor causing osteomalacia: a potential application of PRRT beyond neuroendocrine tumors. J Nucl Med Technol 2016;44(4):248–50.
[36] ten Bokum AM, Hofland LJ, de Jong G, Bouma J, Melief MJ, Kwekkeboom DJ, et al. Immunohistochemical localization of somatostatin receptor sst2A in sarcoid granulomas. Eur J Clin Invest 1999;29(7):630–6.
[37] Tertychnyi AS, Akhrieva KH, Zairat'yants OV, Selivanova LS, Birg TM. Somatostatin receptor expression in the ileal mucosa of patients with inflammatory bowel disease. Arkh Patol 2016;78(1):19–24.
[38] Vanhagen PM, Markusse HM, Lamberts SW, Kwekkeboom DJ, Reubi JC, Krenning EP. Somatostatin receptor imaging. The presence of somatostatin receptors in rheumatoid arthritis. Arthritis Rheum 1994;37(10):1521–7.
[39] Klinaki I, Al-Nahhas A, Soneji N, Win Z. 68Ga DOTATATE PET/CT uptake in spinal lesions and MRI correlation on a patient with neuroendocrine tumor: potential pitfalls. Clin Nucl Med 2013;38(12):e449–53.
[40] Brogsitter C, Hofmockel T, Kotzerke J. (68)Ga DOTATATE uptake in vertebral hemangioma. Clin Nucl Med 2014;39(5):462–3.
[41] Demirci E, Akyel R, Kilic F, Kantarci F, Halac M, Sonmezoglu K. Dual false positive of (6)(8)Ga-DOTA-TATE PET/CT scan in a patient with a history of pancreatic neuroendocrine tumor: a case report. Revista espanola de medicina nuclear e imagen molecular 2015;34(2):133–5.
[42] Walker RC, Smith GT, Liu E, Moore B, Clanton J, Stabin M. Measured human dosimetry of 68Ga-DOTATATE. J Nucl Med 2013;54(6):855–60.
[43] Yu WJ, He JW, Fu WZ, Wang C, Zhang ZL. Reports of 17 Chinese patients with tumor-induced osteomalacia. J Bone Miner Metab. 2017 May;35(3):298–307.
[44] Jiang Y, Xia WB, Xing XP, Silva BC, Li M, Wang O, et al. Tumor-induced osteomalacia: an important cause of adult-onset hypophosphatemic osteomalacia in China: report of 39 cases and review of the literature. J Bone Miner Res Off J Am Soc Bone Miner Res 2012;27(9):1967–75.
[45] Honda R, Kawabata Y, Ito S, Kikuchi F. Phosphaturic mesenchymal tumor, mixed connective tissue type, non-phosphaturic variant: report of a case and review of 32 cases from the Japanese published work. J Dermatol 2014;41(9):845–9.
[46] Jain AS, Shelley S, Muthukrishnan I, Kalal S, Amalachandran J, Chandran S. Diagnostic importance of contrast enhanced (18)F-fluorodeoxyglucose positron emission computed tomography in patients with tumor induced osteomalacia: our experience. Indian J Nucl Med 2016;31(1):14–9.
[47] Costelloe CM, Murphy Jr. WA, Chasen BA. Musculoskeletal pitfalls in 18F-FDG PET/CT: pictorial review. AJR Am J Roentgenol 2009;193(3 Suppl):WS1–13. [Quiz S26-30].
[48] Grigolon MV, Delbeke D. F-18 FDG uptake in a bone infarct: a case report. Clin Nucl Med 2001;26(7):613–4.
[49] Wang M, Zhou L, Xue HD, Jiang Y, Zhong DR, Zhu ZH. Clinical and radiologic characteristics of craniomaxillofacial primary tumor induced osteomalacia: a retrospective analysis. Zhonghua Kou Qiang Yi Xue Za Zhi 2016;51(6):341–5.
[50] Qari H, Hamao-Sakamoto A, Fuselier C, Cheng YS, Kessler H, Wright J. Phosphaturic mesenchymal tumor: 2 new oral cases and review of 53 cases in the head and neck. Head Neck Pathol 2016;10(2):192–200.
[51] Uramoto N, Furukawa M, Yoshizaki T. Malignant phosphaturic mesenchymal tumor, mixed connective tissue variant of the tongue. Auris Nasus Larynx 2009;36(1):104–5.
[52] Metser U, Even-Sapir E. Increased (18)F-fluorodeoxyglucose uptake in benign, nonphysiologic lesions found on whole-body positron emission tomography/computed tomography (PET/CT): accumulated data from four years of experience with PET/CT. Semin Nucl Med 2007;37(3):206–22.
[53] Chang CY, Yang BH, Lin KH, Liu RS, Wang SJ, Shih WJ. Feasibility and incremental benefit of puffed-cheek 18F-FDG PET/CT on oral cancer patients. Clin Nucl Med 2013;38(10):e374–8.
[54] Kumar R, Mukherjee A, Mittal BR. Special techniques in PET/computed tomography imaging for evaluation of head and neck cancer. PET Clin 2016;11(1):13–20.
[55] Kaneuchi Y, Hakozaki M, Yamada H, Hasegawa O, Tajino T, Konno S. Missed causative tumors in diagnosing tumor-induced osteomalacia with (18)F-FDG PET/CT: a potential pitfall of standard-field imaging. Hell J Nucl Med 2016;19(1):46–8.
[56] Shimamoto H, Tatsumi M, Kakimoto N, Hamada S, Shimosegawa E, Murakami S, et al. (18)F-FDG accumulation in the oral cavity is associated with periodontal disease and apical periodontitis: an initial demonstration on PET/CT. Ann Nucl Med 2008;22(7):587–93.
[57] Biagini GL, Coutinho PR, Jonasson TH, Ueda CE, Gama RR. Oncogenic osteomalacia: localization of underlying peripheral tumor with 99mTc-sestamibi scintigraphy. Arq Bras Endocrinol Metabol 2008;52(9):1505–9.
[58] Hodgson SF, Clarke BL, Tebben PJ, Mullan BP, Cooney 3rd WP, Shives TC. Oncogenic osteomalacia: localization of underlying peripheral mesenchymal tumors with use of Tc 99m sestamibi scintigraphy. Endocr Pract 2006;12(1):35–42.
[59] Kimizuka T, Ozaki Y, Sumi Y. Usefulness of 201Tl and 99mTc MIBI scintigraphy in a case of oncogenic osteomalacia. Ann Nucl Med 2004;18(1):63–7.
[60] Adalet I, Ozger H, Cantez S. Comparison of Tc-99m MIBI and Tl-201 uptake in musculoskeletal lesions. Clin Nucl Med 1996;21(2):118–21.
[61] Caner B, Kitapcl M, Unlu M, Erbengi G, Calikoglu T, Gogus T, et al. Technetium-99m-MIBI uptake in benign and malignant bone lesions: a comparative study with technetium-99m-MDP. J Nucl Med 1992;33(3):319–24.
[62] Adalet I, Aktay R, Sirali M, Cantez S, Terzioglu T, Alagol F. Uptake of thallium-201 in brown tumor and bone fractures. Clin Nucl Med 1994;19(6):542–3.
[63] Palaniswamy SS, Subramanyam P, Kumar H. Oncogenic osteomalacia diagnosed by blood pool scintigraphy. Indian J Nucl Med 2011;26(4):188–91.
[64] Satyaraddi A, Cherian KE, Shetty S, Kapoor N, Jebasingh FK, Cherian VM, et al. Musculoskeletal oncogenic osteomalacia-an experience from a single centre in South India. J Orthop 2017;14(1):184–8.
[65] Sood A, Agarwal K, Shukla J, Goel R, Dhir V, Bhattacharya A, et al. Bone scintigraphic patterns in patients of tumor induced osteomalacia. Indian journal of nuclear medicine. IJNM 2013;28(3):173–5.
[66] Duet M, Kerkeni S, Sfar R, Bazille C, Liote F, Orcel P. Clinical impact of somatostatin receptor scintigraphy in the management of tumor-induced osteomalacia. Clin Nucl Med 2008;33(11):752–6.
[67] Halperin F, Anderson RJ, Mulder JE. Tumor-induced osteomalacia: the importance of measuring serum phosphorus levels. Nat Clin Pract Endocrinol Metab 2007;3(10):721–5.
[68] Chong WH, Molinolo AA, Chen CC, Collins MT. Tumor-induced osteomalacia. Endocr Relat Cancer 2011;18(3):R53–77.
[69] Chakraborty PP, Bhattacharjee R, Mukhopadhyay S, Chowdhury S. 'Rachitic rosary sign' and 'tie sign' of the sternum in tumour-induced osteomalacia. BMJ Case Rep 2016;2016.
[70] Wang H, Zhong D, Liu Y, Jiang Y, Qiu G, Weng X, et al. Surgical treatments of tumor-induced osteomalacia lesions in long bones: seventeen cases with more than one year of follow-up. J Bone Joint Surg Am 2015;97(13):1084–94.
[71] Niemeier T, Leddy L, Bolster M, Chapin R. Insufficiency fracture associated with oncogenic osteomalacia. J Clin Rheumatol 2013;19(1):38–42.
[72] Piemonte S, Romagnoli E, Cipriani C, De Lucia F, Pilotto R, Diacinti D, et al. Six-year follow-up of a characteristic osteolytic lesion in a patient with tumor-induced osteomalacia. Eur J Endocrinol 2014;170(1):K1–4.
[73] Umphrey LG, Whitaker MD, Bosch EP, Cook CB. Clinical and bone density outcomes of tumor-induced osteomalacia after treatment. Endocr Pract 2007;13(5):458–62.
[74] Amblee A, Uy J, Senseng C, Hart P. Tumor-induced osteomalacia with normal systemic fibroblast growth factor-23 level. Clin Kidney J 2014;7(2):186–9.
[75] Avila NA, Skarulis M, Rubino DM, Doppman JL. Oncogenic osteomalacia: lesion detection by MR skeletal survey. AJR Am J Roentgenol 1996;167(2):343–5.
[76] Fukumoto S, Takeuchi Y, Nagano A, Fujita T. Diagnostic utility of magnetic resonance imaging skeletal survey in a patient with oncogenic osteomalacia. Bone 1999;25(3):375–7.
[77] Nakanishi K, Sakai M, Tanaka H, Tsuboi H, Hashimoto J, Hashimoto N, et al. Whole-body MR imaging in detecting phosphaturic mesenchymal tumor (PMT) in tumor-induced hypophosphatemic osteomalacia. Magn Reson Med Sci 2013;12(1):47–52.
[78] Hendry DS, Wissman R. Case 165: oncogenic osteomalacia. Radiology 2011;258(1):320–2.
[79] Pithankuakul K, Ratanasuwan T, Thanakit V, Sukhantanak B, Kiatisevi P. Oncogenic osteomalacia caused by phosphaturic mesenchymal tumours in the proximal and shaft of the tibia: a case report. J Orthop Surg (Hong Kong) 2014;22(2):257–62.
[80] Mathis DA, Stehel Jr. EJ, Beshay JE, Mickey BE, Folpe AL, Raisanen J. Intracranial phosphaturic mesenchymal tumors: report of 2 cases. J Neurosurg 2013;118(4):903–7.
[81] Fathalla H, Cusimano M, Di Ieva A, Karamchandani J, Fung R, Kovacs K. Osteomalacia-inducing tumors of the brain: a case report, review and a hypothesis. World Neurosurg 2015;84(1):189 e1–5.

[82] Yavropoulou MP, Gerothanasi N, Frydas A, Triantafyllou E, Poulios C, Hytiroglou P, et al. Tumor-induced osteomalacia due to a recurrent mesenchymal tumor over-expressing several growth factor receptors. Endocrinol Diabetes Metab Case Rep 2015;2015:150025.
[83] Sahoo J, Balachandran K, Kamalanathan S, Das AK, Patro DK, Halanaik D, et al. Tumor(s) induced osteomalacia—a curious case of double trouble. J Clin Endocrinol Metab 2014;99(2):395–8.
[84] Chouhan V, Agrawal K, Vinothkumar TK, Mathesul A. Bilateral insufficiency fracture of the femoral head and neck in a case of oncogenic osteomalacia. J Bone Joint Surg 2010;92(7):1028–31.
[85] Weidner N, Santa Cruz D. Phosphaturic mesenchymal tumors. A polymorphous group causing osteomalacia or rickets. Cancer 1987;59(8):1442–54.
[86] Creytens D, Van Dorpe J. DOG1 expression in phosphaturic mesenchymal tumour. Journal of Clinical Pathology 2016;69:1037–8.
[87] Kimura S, Yanagisawa M, Fujita Y, Sakihara S, Hisaoka M, Kurose A. A case of phosphaturic mesenchymal tumor of the pelvis with vascular invasion. Pathol Int 2015;65(9):510–2.
[88] Uchihashi K, Nishijima-Matsunobu A, Matsuyama A, Yamasaki F, Tanabe T, Uemura T, et al. Phosphaturic mesenchymal tumor, nonphosphaturic variant, causing fatal pulmonary metastasis. Hum Pathol 2013;44(11):2614–8.
[89] Qiu S, Cao LL, Qiu Y, Yan P, Li ZX, Du J, et al. Malignant phosphaturic mesenchymal tumor with pulmonary metastasis: a case report. Medicine (Baltimore) 2017;96(17):e6750.
[90] Tutton S, Olson E, King D, Shaker JL. Successful treatment of tumor-induced osteomalacia with CT-guided percutaneous ethanol and cryoablation. J Clin Endocrinol Metab 2012;97(10):3421–5.
[91] Jadhav S, Kasaliwal R, Shetty NS, Kulkarni S, Rathod K, Popat B, et al. Radiofrequency ablation, an effective modality of treatment in tumor-induced osteomalacia: a case series of three patients. J Clin Endocrinol Metab 2014;99(9):3049–54.
[92] Hesse E, Rosenthal H, Bastian L. Radiofrequency ablation of a tumor causing oncogenic osteomalacia. N Engl J Med 2007;357(4):422–4.
[93] Tella SH, Amalou H, Wood BJ, Chang R, Chen CC, Robinson C, et al. Multimodality image-guided cryoablation for inoperable tumor-induced osteomalacia. J Bone Miner Res Off J Am Soc Bone Miner Res 2017;32(11):2248–56.
[94] Sekine T, Barbosa FG, Sah BR, Mader CE, Delso G, Burger IA, et al. PET/MR outperforms PET/CT in suspected occult tumors. Clin Nucl Med 2017;42(2):e88–95.
[95] Hope TA, Pampaloni MH, Nakakura E, VanBrocklin H, Slater J, Jivan S, et al. Simultaneous (68)Ga-DOTA-TOC PET/MRI with gadoxetate disodium in patients with neuroendocrine tumor. Abdom Imaging 2015;40(6):1432–40.